THE JOURNAL OF BIOLOGICAL CHEMISTRY VOL. 284, NO. 7, pp. 4658–4666, February 13, 2009

Interferon-γ Targets Cancer Cells and Osteoclasts to Prevent Tumor-associated Bone Loss and Bone Metastases*[S]

Received for publication, June 24, 2008, and in revised form, October 27, 2008 Published, JBC Papers in Press, December 5, 2008, DOI 10.1074/jbc.M804812200

Zhiqiang Xu[‡1], Michelle A. Hurchla[‡1], Hongju Deng[‡], Özge Uluçkan[‡], Fang Bu[‡], Andrew Berdy[‡], Mark C. Eagleton[‡], Emanuela A. Heller[‡], Desiree H. Floyd[‡], Wessel P. Dirksen[§], Sherry Shu[§], Yuetsu Tanaka[¶], Soledad A. Fernandez[‖], Thomas J. Rosol[§], and Katherine N. Weilbaecher[‡2]

From the [‡]Department of Medicine, Division of Oncology, Washington University School of Medicine, St. Louis, Missouri 63110, the [§]Department of Veterinary Biosciences, Ohio State University, Columbus, Ohio 43210, the [¶]Department of Immunology, Graduate School and Faculty of Medicine, University of the Ryukyus, Okinawa 903-0213, Japan, and the [‖]Center for Biostatistics, Ohio State University, Columbus, Ohio 43210

Interferon-γ (IFN-γ) has been shown to enhance anti-tumor immunity and inhibit the formation of bone-resorbing osteoclasts. We evaluated the role of IFN-γ in bone metastases, tumor-associated bone destruction, and hypercalcemia in human T cell lymphotrophic virus type 1-Tax transgenic mice. Compared with $Tax^+IFN\text{-}\gamma^{+/+}$ mice, $Tax^+IFN\text{-}\gamma^{-/-}$ mice developed increased osteolytic bone lesions and soft tissue tumors, as well as increased osteoclast formation and activity. *In vivo* administration of IFN-γ to tumor-bearing $Tax^+IFN\text{-}\gamma^{-/-}$ mice prevented new tumor development and resulted in decreased bromodeoxyuridine uptake by established tumors. *In vitro*, IFN-γ directly decreased the viability of Tax^+ tumor cells through inhibition of proliferation, suppression of ERK phosphorylation, and induction of apoptosis and caspase 3 cleavage. IFN-γ also inhibited macrophage colony-stimulating factor-mediated proliferation and survival of osteoclast progenitors *in vitro*. Administration of IFN-γ to C57BL/6 mice decreased Tax^+ tumor growth and prevented tumor-associated bone loss and hypercalcemia. In contrast, IFN-γ treatment failed to protect $IFN\text{-}\gamma R1^{-/-}$ mice from Tax^+ tumor-induced skeletal complications, despite decreasing tumor growth. These data demonstrate that IFN-γ suppressed tumor-induced bone loss and hypercalcemia in Tax^+ mice by inhibiting both Tax^+ tumor cell growth and host-induced osteolysis. These data suggest a protective role for IFN-γ in patients with bone metastases and hypercalcemia of malignancy.

IFN-γ[3] is a multifunctional cytokine produced mainly by NK cells and activated T cells that plays a critical role in host immune responses against pathogens and cancer (1). Mice deficient in IFN-γ, the R1 subunit of the IFN-γ receptor, or the transcription factor STAT1 are more susceptible to spontaneous tumor development (1–3). IFN-γ has also been found to have direct anti-proliferative and pro-apoptotic effects on tumor cells in animal models (4, 5); however, administration of high dose IFN-γ to patients with advanced renal and ovarian cancer has had only limited success and failed to improve overall survival (1, 6).

IFN-γ has been shown to regulate bone cell differentiation and function with complex effects on skeletal health. However, the role of IFN-γ in pathological bone disease is largely controversial. Previously, it has been reported that IFN-γ can inhibit the critical osteoclast regulator, receptor activator of NFκB ligand (RANKL), by activating ubiquitin-mediated degradation of its signaling pathway adaptor protein TRAF-6 (7, 8). Mice deficient for IFN-γ or its receptor develop enhanced bone loss associated with collagen-induced arthritis (9–11). In contrast, Gao *et al.* (12) recently found that IFN-γ indirectly stimulates osteoclast formation and bone loss after ovariectomy via antigen-driven T cell activation, resulting in the production of osteoclast-activating factors. Interestingly, IFN-γ has been used to treat infantile osteopetrosis in which patients suffered from high bone mass secondary to osteoclast dysfunction or osteoblast hyperactivity, but the mechanism of action may be through modulation of the host immune system rather than direct effects on bone cells (13–15). However, the role of IFN-γ in the treatment of osteolytic bone metastases has not been elucidated.

We evaluated the effects of IFN-γ in HTLV-1-Tax transgenic mice that develop osteolytic bone tumors and hypercalcemia (16, 17). Previously, it was shown that $HTLV\text{-}1\text{-}Tax^+IFN\text{-}\gamma^{-/-}$ mice develop increased numbers of soft tissue tumors with enhanced tumor-associated angiogenesis and up-regulation of vascular endothelial growth factor expression; however, the impact on bone metastases and hypercalcemia in these mice

* This work was supported, in whole or in part, by National Institutes of Health Grants PPG CA100730 and R01 CA 097250 (to Z. X., M. H., H. D., M. C. E., D. H. F., E. A. H., and K. N. W.), Grant T32 CA09547 (cancer biology training grant to O. U. and M. H.), and Grant RO1 CA100730 (to T. J. R. and W. P. D. and NCRR to S. S.), as well as by the St. Louis Men's Club Against Cancer (to K. N. W.). The costs of publication of this article were defrayed in part by the payment of page charges. This article must therefore be hereby marked "*advertisement*" in accordance with 18 U.S.C. Section 1734 solely to indicate this fact.

[S] The on-line version of this article (available at http://www.jbc.org) contains supplemental Experimental Procedures and Figs. 1 and 2.

[1] Both authors contributed equally to this work.

[2] To whom correspondence should be addressed: 660 S. Euclid Ave, Campus Box 8069, Washington University School of Medicine, St. Louis, MO 63110. Tel.: 314-454-8973; Fax: 314-454-8979; E-mail: kweilbae@dom.wustl.edu.

[3] The abbreviations used are: IFN-γ, interferon-γ; BrdUrd, bromodeoxyuridine; HTLV-1, human T cell lymphotrophic virus, type 1; M-CSF, macrophage colony-stimulating factor; RANKL, receptor activator of NFκB ligand; ANOVA, analysis of variance; BMM, bone marrow-derived macrophage; OC, osteoclast; MTT, 3-(4,5-dimethylthiazol-2-yl)-2,5-diphenyltetrazolium bromide; RT, reverse transcription; DAPI, 4′,6-diamidino-2-phenylindole; MEK, mitogen-activated protein kinase kinase; BMM, bone marrow-derived macrophage; TRAP, tartrate-resistant acid phosphatase; PTHrP, parathyroid hormone-related protein; STAT, signal transducers and activators of transcription; BMD, bone mineral density; DXA, dual energy x-ray absorptiometry; HHM, humeral hypercalcemia of malignancy.

was not evaluated (2). Because of the multiple complex effects of IFN-γ on osteoclasts, anti-tumor and anti-viral immunity, we hypothesized that IFN-γ would affect tumor-associated bone destruction and bone metastases in HTLV-1-Tax transgenic mice. In this study, we demonstrate enhanced osteolytic bone disease and increased osteoclast activity in $Tax^{+}IFN\text{-}\gamma^{-/-}$ mice as compared with $Tax^{+}IFN\text{-}\gamma^{+/+}$ mice. We show that IFN-γ directly inhibited the growth of Tax-expressing tumor cells by suppressing their proliferation and inducing apoptosis. IFN-γ was also able to directly inhibit *in vitro* osteoclast formation in Tax^{+} mice. In summary, treatment with IFN-γ resulted in decreased tumor growth and prevented tumor-associated bone loss and hypercalcemia in $Tax^{+}IFN\text{-}\gamma^{-/-}$ mice.

EXPERIMENTAL PROCEDURES

Animals—HTLV-1-Tax transgenic mice (Tax^{+}) (16), $IFN\text{-}\gamma R1^{-/-}$ mice, and $IFN\text{-}\gamma^{-/-}$ mice all on a C57BL/6 background were gifts from Dr. Lee Ratner, Dr. Robert Schreiber, and Dr. Skip Virgin, respectively, at Washington University School of Medicine. C57BL/6 mice were obtained from Harlan Labs (Indianapolis, IN). Mice were housed under pathogen-free conditions according to the guidelines of the Division of Comparative Medicine, Washington University School of Medicine. The animal ethics committee of Washington University School of Medicine approved all experiments.

Radiography—Osteolytic lesion formation was monitored by serial x-ray imaging (Faxitron, Buffalo Grove, IL). Bone mineral density, by Dual Energy X-ray Absorptiometry (DXA), was measured and analyzed by a PIXImus2 scanner according to the manufacturer's protocol (Lunar Corp., Madison, WI).

Serum Bone Turnover Markers—Serum tartrate-resistant acid phosphatase (TRAP), a marker of osteoclast number, was measured using a quantitative TRAP solution assay (modified from Tintut *et al.* (18)), which was performed by adding a colorimetric substrate, 5.5 mM *p*-nitrophenyl phosphate, in the presence of 10 mM sodium tartrate at pH 4.5. The reaction product was quantified by measuring absorbance at 405 nm. Serum calcium was corrected for albumin concentration.

$Tax^{+}IFN\text{-}\gamma^{-/-}$ Tumor Cell Line (TGN), Tumor Transplantation, and in Vivo IFN-γ Treatment—TGN ($\underline{T}ax^{+}$ interferon-$\underline{\gamma}$ $\underline{n}$ull) tumor cell line was isolated from a spontaneous subcutaneous tumor that arose in a $Tax^{+}IFN\text{-}\gamma^{-/-}$ mouse (supplemental Fig. 1 and supplemental Experimental Procedures). For tumor transplantation, 1×10^{6} TGN cells were resuspended in 200 μl of Matrigel (1:1 dilution with phosphate-buffered saline; BD Biosciences) and implanted subcutaneously in the lower dorsal region of the mice as described previously (19). Murine recombinant IFN-γ (PeproTech, Rocky Hill, NJ) or normal saline (vehicle) was administered via intraperitoneal injection at a dose of 10^{6} units/kg in 200 μl of saline, three times/week starting on the same day as tumor inoculation and continuing for 3–4 weeks. Tumor volume in the living mouse was measured using bidirectional precision caliper measurements $((4/3\pi \cdot \text{length}/2 \cdot (\text{width}/2)^{2})$.

Bone Histomorphometry and Immunohistochemistry—Mouse tibias were fixed in formalin, decalcified in 14% EDTA for 2 weeks, and then processed and stained for TRAP as described previously (19, 20). OC numbers, OC perimeter, bone marrow space, and bone erosion were measured according to a standard protocol as described previously, using Image-Pro Plus, version 5.0 software (Media Cybernetics, Bethesda) (19). Peripheral soft tumor, visceral metastatic tumor, and mouse bone samples were processed as described previously (17). For *in vivo* BrdUrd labeling, 200 μl of 1 mg/ml BrdUrd (Pharmingen) dissolved in phosphate-buffered saline was injected intraperitoneally into mice 24 h before mice necropsy. Paraffin-embedded tissue sections from labeled tumor tissues were stained with BrdUrd antibody (BD Biosciences) by standard ABC method. Immunohistochemistry staining was done by routine ABC method according to protocol (available on line). Antigen retrieval was done using microwave heating method with 10 mM sodium citrate buffer (pH 6, DAKO). Anti-Tax monoclonal antibody (gift of Dr. Tanaka) (21) was used at 1:100 for immunohistochemistry and immunofluorescence and 1:1000 for Western blotting. For immunofluorescence staining, biotin-labeled secondary antibody combined with phycoerythrin-conjugated streptavidin (Molecular Probes, Carlsbad, CA) was used. Nuclei were counterstained by DAPI. Images were collected using a Nikon Eclipse TE300 microscope equipped with a plan Fluor lens and a magnafire camera (Optronics, Goleta, CA).

Reverse Transcription PCR—RNA was isolated from tumor cells or OC using the Qiagen RNeasy mini kit (Qiagen, Valencia, CA) according to manufacturer's protocols. RT-PCR was performed using an Invitrogen kit as described previously (17). Primers specific for mouse IFN-γ receptor were synthesized by IDT, and the sequences are as follows: mouse IFN-γ receptor forward, 5′-CAAATACCAGGATAACTACTG-3′, and mouse IFN-γ receptor reverse, 5′-CGAAAGACGTCTG-TATCCCTC-3′. HTLV-1-Tax primer and glyceraldehyde-3-phosphate dehydrogenase primers were described previously (17, 22).

Cell Viability, Proliferation, and Apoptosis Assays—TGN cells or BMMs were plated at 3000 cells/well in 96-well plate in RPMI 1640 media containing 10% fetal bovine serum or 10% fetal bovine serum/α-minimum Eagle's medium respectively and then incubated with different doses of recombinant murine IFNγ (PeproTech, Rocky Hill, NJ) for 24–72 h. For BrdUrd labeling, BMMs or TGN cells were first serum-starved for 2 h before adding IFN-γ. MTT (Sigma) and BrdUrd cell proliferation assay (Roche Applied Science) were performed as described previously (19) according to the manufacturer's instruction. Where described, 20 μM U0126 MEK1/2 inhibitor (Cell Signaling Technology, Danvers, MA) was added to cells for 4 h prior to addition of IFN-γ. For annexin-V staining TGN cells were plated at 6×10^{4} cells/ml in 12-well plates, serum-starved for 2 h, followed by IFN-γ treatment for 48 h. Cells were stained with annexin-V-fluorescein isothiocyanate and 7-amino-actinomycin D (BD Biosciences) according to the manufacturer's protocols. Data were collected on a FACSCalibur (BD Biosciences) and analyzed with FlowJo (Treestar, Ashland, OR).

Macrophage and Osteoclast Formation Assays—Whole bone marrow was extracted from femurs and tibias of Tax^{+} mice (6–8 weeks old), and *in vitro* osteoclast formation was done as

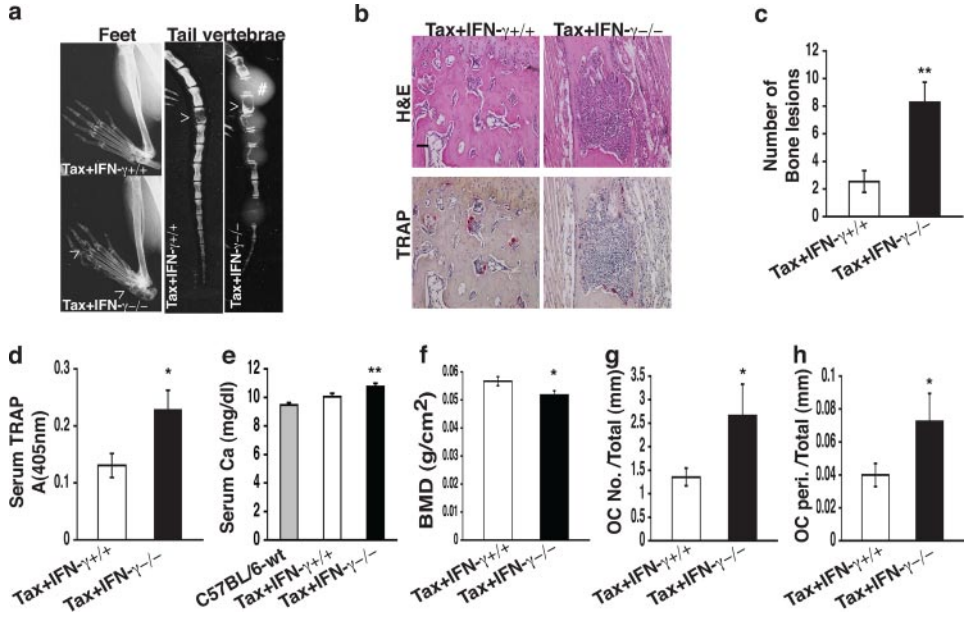

FIGURE 1. **Increased osteolytic lesion formation and enhanced osteoclast activity in Tax$^+$IFN-$\gamma^{-/-}$ mice.** *a*, representative x-rays of feet and tail vertebrae (<, osteolytic bone lesion; #, peripheral soft tumor). *b*, hematoxylin and eosin (*H&E*) and TRAP stains on longitudinal sections of tail vertebrae. *c*, quantification of number of bone lesions by x-ray (**, $p < 0.01$ by Wilcoxon rank sum test; $n = 16$; Tax$^+$IFN-$\gamma^{+/+}$; $n = 15$; Tax$^+$IFN$\gamma^{-/-}$). *d*, serum TRAP activity as measured by TRAP solution assay (*, $p < 0.05$ by Wilcoxon rank sum test; $n = 13$; Tax$^+$IFN-$\gamma^{+/+}$ $n = 11$; Tax$^+$IFN-$\gamma^{-/-}$). *e*, serum calcium level corrected for serum albumin (**, $p < 0.01$ $n = 13$; Tax$^+$IFN-$\gamma^{+/+}$; $n = 11$; Tax$^+$IFN-$\gamma^{-/-}$). *f*, BMD of femurs from 9-month-old mice as measured by DXA analysis (*, $p < 0.05$ $n = 13$; Tax$^+$IFN-$\gamma^{+/+}$; $n = 11$; Tax$^+$IFN-$\gamma^{-/-}$). *g* and *h*, histomorphometric analysis of (*g*) osteoclast number and (*h*) osteoclast perimeter measured from tail vertebrae of Tax$^+$IFN-$\gamma^{+/+}$ and Tax$^+$IFN-$\gamma^{-/-}$ mice (*, $p < 0.05$). *e–h* were analyzed by ANOVA.

described previously (19, 23). TRAP staining was performed according to the manufacturer's instructions (Sigma), and the number of TRAP-positive cells with three or more nuclei in five 4× fields was counted blinded to genotype.

Cell Signaling and Immunoblotting—TGN cells were plated in 6-well plates, serum-starved for 2 h, and treated with different doses of IFN-γ in RPMI 1640 media containing 10% fetal bovine serum for 1–72 h. Protein lysates were harvested in RIPA buffer (Sigma) containing protease inhibitors mixture (Roche Applied Science) and then quantified by BCA method (Pierce). Total of 40 μg of protein was electrophoresed and blotted with relevant antibodies by immunoblot analysis. For phospho-AKT, rabbit monoclonal antibody was from Covance Research Products (Princeton, NJ) at 1:250; and all other antibodies were ordered from Cell Signaling (Danvers, MA), including the following: total AKT, polyclonal, 1:1000; total ERK, polyclonal, 1:1000; total STAT1, polyclonal, 1:1000; phospho-STAT1, polyclonal, 1:1000; phospho-ERK, monoclonal, 1:1000; and anti-caspase-3 antibody, 1:500. Anti-Tax monoclonal antibody was a gift from Dr. Tanaka and used at a 1:1000 dilution (21).

Statistical Analyses—Several experiments were reported in this study, and different outcome variables were measured. Thus, different statistical methods were used to test the association between outcome variables and groups depending on the sample sizes, and sampling distributions of the outcome variables were involved in these comparisons. In general, when sample sizes were small and/or the variances in the different treatment groups were not homogeneous, nonparametric tests were used (two-sample Wilcoxon rank-sum (Mann-Whitney)). Wilcoxon rank-sum test was used to compare peripheral soft tumor incidence, serum TRAP, and rate of osteolytic lesion formation between the two mice groups. ANOVA and two-sample Student's *t* tests were used to compare histomorphometric outcome variables, *in vitro* viability and proliferation, serum calcium levels, and BMD. ANOVA with repeated measures was used to compare tumor volume across time between treated *versus* control mice (Fig. 2*a* and Fig. 5*e*). For these repeated measures, ANOVA models take into account the correlations of measurements within same mice. The Bonferroni method was used to adjust for multiplicity when pairwise comparisons were performed. Differences were considered statistically significant when the *p* value was <0.05.

RESULTS

Increased Osteolytic Tumor Formation and Osteoclast Activity in Tax$^+$IFN-$\gamma^{-/-}$ Mice—Tax transgenic mice were crossed with IFN-$\gamma^{-/-}$ mice to generate Tax$^+$IFN-$\gamma^{-/-}$ mice. Consistent with previous observations (2), we found that Tax$^+$IFN-$\gamma^{-/-}$ mice formed increased numbers of peripheral soft tissue tumors by 6 months as compared with Tax$^+$IFN-$\gamma^{+/+}$ (71 *versus* 28% respectively, $p < 0.005$). 89% of 6-month-old Tax$^+$IFN-$\gamma^{-/-}$ mice also had x-ray evidence of osteolytic skeletal tumors compared with 50% in age-matched Tax$^+$IFN-$\gamma^{+/+}$ mice ($p < 0.05$). By 9 months, Tax$^+$IFN-$\gamma^{-/-}$ mice also revealed significant increases in the number of osteolytic bone lesions (Fig. 1, *a–c*). In addition to osteolytic lesions in the tail vertebrae, Tax$^+$IFN-$\gamma^{-/-}$ also developed osteolytic lesions in the appendicular skeleton, which were a rare occurrence in Tax$^+$IFN-$\gamma^{+/+}$ mice (Fig. 1*a*). Increased numbers of tartrate-resistant acid phosphatase (TRAP)-expressing OCs were present in the tail vertebrae of Tax$^+$IFN-$\gamma^{-/-}$ mice (Fig. 1*b*). Serum levels of the OC marker, TRAP, were significantly higher in Tax$^+$IFN-$\gamma^{-/-}$ mice consistent with increased OC activity *in vivo* (Fig. 1*d*). Also suggesting increased OC activity, Tax$^+$IFN-$\gamma^{-/-}$ mice had significantly elevated serum calcium compared with non-Tax transgenic wild type (WT) age-matched historical controls (Fig. 1*e*). Evaluation of BMD as measured by DXA analysis demonstrated decreased BMD in the femur of tumor-bearing Tax$^+$IFN-$\gamma^{-/-}$ mice compared with Tax$^+$IFN-$\gamma^{+/+}$ mice (Fig. 1*f*). Histomorphometric analysis of tail vertebrae demonstrated a significant increase in OC numbers and OC perimeters covering the bone surface (Fig. 1, *g* and *h*). These data show that, compared with Tax$^+$IFN-$\gamma^{+/+}$ mice, Tax$^+$IFN-$\gamma^{-/-}$ mice developed increased numbers of osteo-

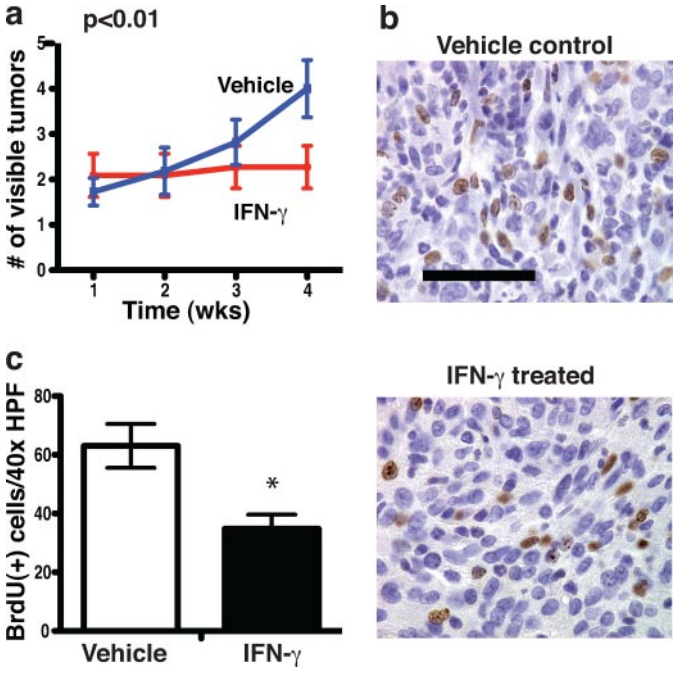

FIGURE 2. **Recombinant IFN-γ treatment prevented new tumor formation in Tax$^+$IFN-γ$^{-/-}$ mice.** *a,* average number of visible soft tissue tumor in Tax$^+$IFN-γ$^{-/-}$ mice treated with vehicle or recombinant IFN-γ measured weekly for 4 weeks, $p < 0.01$ by repeated measures ANOVA (vehicle, $n = 11$; IFN-γ, $n = 11$). *b,* representative BrdUrd labeling of soft tissue tumors from Tax$^+$ IFN-γ$^{-/-}$ mice after 4 weeks of treatment with recombinant IFN-γ or vehicle control. (*Bar,* 50 μm). *c,* average number of BrdUrd-labeled cells counted per ×40 high powered field. $n = 6$ IFN-γ-treated tumors and $n = 8$ vehicle (saline)-treated tumors analyzed with three high powered fields per tumor were analyzed (*, $p < 0.05$ by Student's *t* test).

lytic tumors with increased tumor-associated bone loss and OC activity.

IFN-γ Prevented New Tumor Formation in Tax$^+$ IFN-γ$^{-/-}$ Mice—To evaluate the effects of recombinant murine IFN-γ on tumor growth and formation *in vivo*, tumor bearing Tax$^+$IFN-γ$^{-/-}$ mice received either IFN-γ or saline for 1 month. Mice administered IFN-γ developed significantly fewer new tumors over the course of 1 month of treatment compared with saline controls (Fig. 2*a*). There were no visible differences in the size of established tumors between the two groups during the treatment period; however, *in vivo* BrdUrd labeling showed a significant decrease in BrdUrd uptake by soft tissue tumors (Fig. 2, *b* and *c*). These data demonstrate that recombinant IFN-γ administration decreased new soft tissue tumor formation and decreased the proliferation rate of established tumors in tumor-bearing Tax transgenic mice.

IFN-γ Directly Inhibited Growth of Tax$^+$ Tumor Cells in Vitro—IFN-γ has been reported to directly decrease tumor cell proliferation *in vitro* (4, 24, 25). We hypothesized that the increased tumor burden in Tax$^+$IFN-γ$^{-/-}$ mice was due in part to the lack of IFN-γ-mediated inhibition of tumor growth *in vivo*. To test this hypothesis, we developed a Tax-expressing cell line from a tumor that spontaneously arose in a Tax$^+$IFN-γ$^{-/-}$ mouse. Although this tumor line does not have the ability to produce IFN-γ, it does retain the signaling pathway necessary to respond to the cytokine. Preliminary observations showed that the TGN cells were tumorigenic, highly metastatic, and demonstrated significant pro-osteoclastogenic capabilities, which recapitulates many of the biological behaviors of spontaneous tumors in HTLV-1-Tax transgenic mice (supplemental Fig. 1). We therefore used TGN cells to evaluate the direct anti-tumor effect of IFN-γ, independent of its actions on host cells. TGN cells express IFN-γ receptor by RT-PCR analysis at a similar level to a Tax$^+$IFN-γ$^{+/+}$ tumor line (Tax$^+$ interferon-γ positive; TGP) (Fig. 3*a*). IFN-γ treatment significantly decreased TGN cell viability *in vitro* as measured by MTT assay and inhibited proliferation of TGN cells by BrdUrd incorporation assay (Fig. 3, *b* and *c*). This effect was not dependent on the intrinsic ability of the cells to produce IFN-γ, as TGP cells also exhibited decrease viability following IFN-γ treatment (supplemental Fig. 2).

IFN-γ dose-dependently induced phosphorylation of the canonical IFN-γ transcription factor, STAT1, in TGN cells (Fig. 3*d*). The phosphorylation of STAT1 suggests that the proximal components of the canonical IFN-γ signaling pathway remain functional in this tumor cell line. IFN-γ treatment also decreased ERK phosphorylation in a dose-dependent manner (Fig. 3*d*). This decrease was consistent with our BrdUrd data (Fig. 3*c*) as ERK phosphorylation is associated with cell cycle progression and cell proliferation. To examine if the ERK pathway was responsible for the decrease in TGN viability following IFN-γ treatment, we cultured cells in the presence of the MEK1/2 inhibitor U0126. As a selective inhibitor of the kinase activity of the mitogen-activated protein kinase kinase (MEK), U0126 resulted in downstream inhibition of ERK (26) In the absence of IFN-γ treatment, U0126 decreased the viability of TGN cells, suggesting that ERK phosphorylation was required for their viability (Fig. 3*e*). IFN-γ treatment in the presence of U0126 further decreased the viability of TGN cells (Fig. 3*e*). The additive effect of U0126 and IFN-γ suggested that the decrease in TGN viability cannot be attributed solely to decreased ERK phosphorylation.

We next investigated if IFN-γ may also be causing apoptosis of TGN cells. Microscopically, DAPI staining of IFN-γ-treated TGN cells showed conspicuous DNA fragmentation (Fig. 3*f*). IFN-γ also induced a dose-dependent increase in the cleavage and activation of caspase-3 (Fig. 3*g*). Additionally, TGN cells treated with IFN-γ exhibited increased annexin-V staining as compared with untreated cells (Fig. 3*h*). Annexin-V staining detects phosphatidylserine expression on the outer cell membrane, a marker of apoptosis. We also observed a modest decrease in the phosphorylation of Akt, a mediator of cell survival (Fig. 3*d*). These results demonstrate that IFN-γ can directly affect the viability and proliferation of Tax-expressing tumor cells *in vitro* with associated attenuation of ERK phosphorylation and caspase-3-mediated apoptosis.

Enhanced Osteoclast Formation in Tax$^+$IFN-γ$^{-/-}$ Mice—The enhanced *in vivo* osteoclast activity observed in Tax$^+$IFN-γ$^{-/-}$ (Fig. 1) mice may be due to increased tumor-associated OC formation in these mice. To investigate whether there was a difference in *in vitro* OC formation between Tax$^+$IFN-γ$^{+/+}$ mice and Tax$^+$IFN-γ$^{-/-}$ mice, osteoclasts were generated from BMMs (19). BMMs from Tax$^+$IFN-γ$^{-/-}$ mice formed increased numbers of multinucleated TRAP(+) OCs with higher numbers of nuclei compared with Tax$^+$IFN-γ$^{+/+}$ mice (Fig. 4, *a* and *b*). Previously it has been shown that IFN-γ can

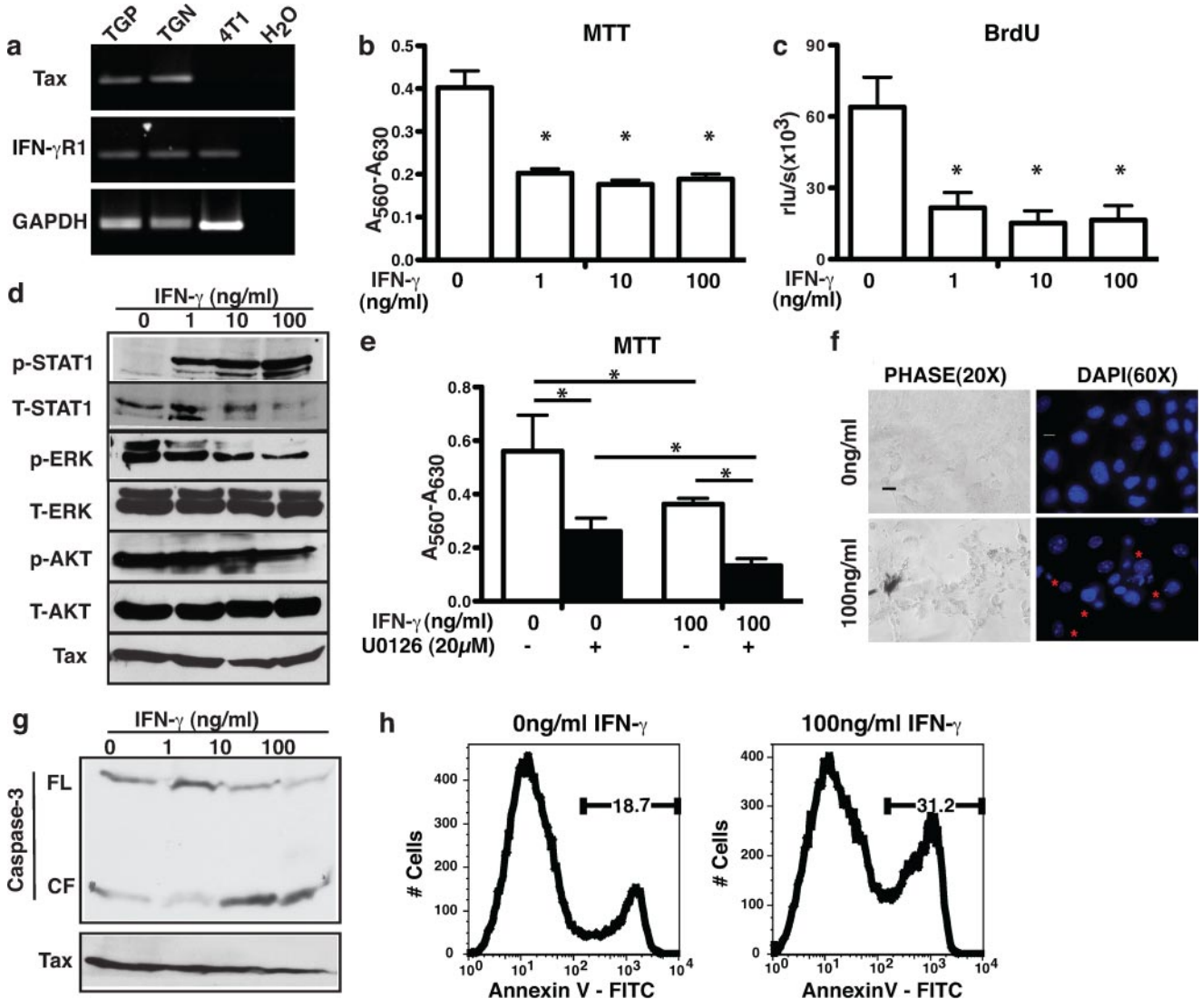

FIGURE 3. **IFN-γ directly inhibited Tax$^+$IFN-γ tumor cells *in vitro*.** *a,* Tax$^+$IFN-$\gamma^{+/+}$ (*TGP*) and Tax$^+$IFN-$\gamma^{-/-}$ (*TGN*) tumor cells express similar levels of the IFN-γ receptor by RT-PCR. *4T1*, a non-Tax expressing murine mammary carcinoma line, is shown as a control. *b* and *c,* IFN-γ treatment of TGN cells for 24 h decreased viability as measured by MTT ($p < 0.01$, ANOVA) (*b*) and decreased proliferation as measured by BrdUrd incorporation ($p < 0.01$, ANOVA) (*c*). *d,* Western blotting of phosphorylated (*p-*) and total (*T-*) STAT1, ERK, and AKT in TGN cells administered IFN-γ for 24 h. Tax protein expression served as loading control. *e,* viability of TGN cells is partially dependent on ERK signaling. *U0126*, a MEK1/2 inhibitor was added to TGN cells 4 h prior to IFN-γ treatment. Cell viability was measured by MTT assay after 48 h of IFN-γ treatment ($p < 0.05$, ANOVA). *f,* phase contrast (*left panel*, ×20 objective) and DAPI staining of IFN-γ treated TGN cells (* mark fragmented nuclei). *g,* Western blotting of caspase 3 in TGN cells treated with IFN-γ for 24 h. Tax expression serves as a loading control. *FL* = full-length and *CF* = cleaved (active) form. *h,* TGN cells undergo apoptosis following 48 h of IFN-γ treatment as shown by an increased percentage of annexin-V-positive cells.

directly inhibit *in vitro* OC formation (8, 27, 28). In Tax$^+$IFN-$\gamma^{-/-}$ and Tax$^+$IFN-$\gamma^{+/+}$ mice, *in vitro* OC formation was significantly inhibited in a dose-dependent fashion by IFN-γ treatment (Fig. 4*c*), whereas OC formation for BMMs isolated from IFN-γR$^{-/-}$ cells were not affected (data not shown). Consistent with this observation, both Tax$^+$IFN-$\gamma^{+/+}$ and Tax$^+$IFN-$\gamma^{-/-}$ OC expressed a similar level of IFNγR1 by RT-PCR (Fig. 4*d*). To further investigate the molecular mechanism responsible for this inhibitory effect, we tested the effects of IFN-γ on proliferation of osteoclast progenitors (BMM). Treating Tax$^+$IFN-$\gamma^{-/-}$ M-CSF-stimulated BMMs with low doses of exogenous IFN-γ resulted in decreased proliferation as measured by BrdUrd uptake (Fig. 4*e*). These data demonstrate that Tax$^+$IFN-$\gamma^{-/-}$ mice display enhanced OC formation and that IFN-γ can directly inhibit OC formation *in vitro* and inhibit M-CSF-mediated proliferation of osteoclast progenitors.

IFN-γ Administration Directly Inhibited Tumor Growth in Vivo and Prevented Tumor-associated Bone Loss and Hypercalcemia—To test whether IFN-γ could directly inhibit tumor growth and establishment *in vivo*, the Tax$^+$IFN-$\gamma^{-/-}$ TGN tumor cell line was subcutaneously implanted into syngeneic immunocompetent C57BL/6 mice. Mice were divided into two groups and treated with vehicle or IFN-γ for 3 weeks. Tumor growth in the IFN-γ-treated mice was significantly decreased as compared with vehicle control (Fig. 5, *a* and *b*). Mice administered IFN-γ also had decreased serum calcium (Fig. 5*c*) and decreased bone loss as measured by DXA (Fig. 5*d*). Because IFN-γ also plays an important role in anti-tumor

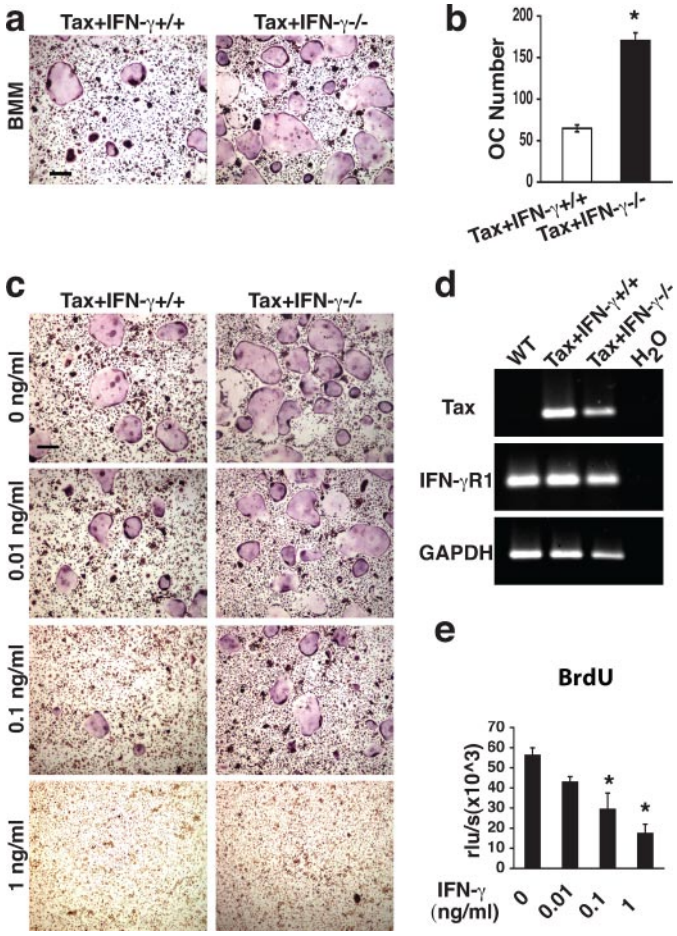

FIGURE 4. **Enhanced osteoclast formation in Tax^{+}IFN-$\gamma^{-/-}$ mice.** *a,* TRAP staining of OC formation from BMMs after 5 days of culture in M-CSF and RANKL (*bar,* 50 μm). *b,* quantification of *in vitro* OC numbers generated from BMMs (*, $p < 0.05$, ANOVA). *c,* IFN-γ dose-dependently inhibited OC formation *in vitro*. TRAP stain after 5 days of BMMs cultured with M-CSF and RANKL (*bar,* 50 μm). *d,* Tax^{+}IFN-$\gamma^{+/+}$ and Tax^{+}IFN-$\gamma^{-/-}$ OC express the IFN-γR. RNA was isolated from day 6 OC grown as in *a* and subjected to RT-PCR for Tax, IFN-γR1, and glyceraldehyde-3-phosphate dehydrogenase (*GAPDH*). *e,* IFN-γ treatment inhibits M-CSF-mediated proliferation of BMMs *in vitro* by BrdUrd incorporation (*, $p < 0.01$, ANOVA).

immune responses (1), it is possible that the inhibition of tumor growth observed in IFN-γ treated mice could be a result of the stimulatory effect of IFN-γ on the host immune system rather than solely through direct inhibition of TGN tumor cell growth.

To differentiate between IFN-γ actions on the tumor cells and on the host cells, we subcutaneously implanted IFN-γ-responsive TGN tumor cells into IFN-γ receptor-deficient (IFN-γR1$^{-/-}$) mice that have IFN-γ unresponsive host cells. We found that IFN-γ treatment abrogated TGN tumor growth in these mice (Fig. 5*e*), confirming that IFN-γ directly acts on the tumor cells, as host cells in IFN-γR1$^{-/-}$ mice are unable to bind and respond to the cytokine. However, IFN-γ administration did not affect serum calcium levels or tumor-associated bone loss in mice lacking IFN-γR1 (Fig. 5, *f* and *g*). These results suggest that IFN-γ modulates tumor-associated bone loss and hypercalcemia by directly targeting host-derived cells. Together these results indicate IFN-γ directly acts on both tumor cells and host-derived cells to block tumor growth and the skeletal complications of malignancy, respectively.

DISCUSSION

Targeted disruption of interferon-γ in HTLV-1-Tax transgenic mice resulted in increased osteolytic tumor formation, osteoclast activation, and increased tumor-associated bone loss. Treating tumor-bearing Tax^{+}IFN-$\gamma^{-/-}$ mice with IFN-γ decreased the formation of new tumors as well as decreased BrdUrd incorporation by existing tumors. IFN-γ administration also inhibited the formation of osteoclasts from bone marrow-derived macrophages and directly inhibited the viability and growth of a Tax-expressing tumor cell line (TGN) *in vitro*. In immunocompetent mice, growth of the TGN tumor line and tumor-associated complications (hypercalcemia and bone loss) were significantly suppressed by IFN-γ treatment. Finally, IFN-γ administration failed to protect IFN-γ receptor-deficient mice challenged with the TGN tumor from the skeletal complications of tumor despite having decreased tumor burden. These results suggest that IFN-γ has two modes of action in experimental models of bone metastases. First, IFN-γ can inhibit tumor growth through direct effects on tumor cells. Second, IFN-γ decreases skeletal complications of malignancy by directly acting on host cells to modulate osteoclast function. To our knowledge, this is the first report demonstrating both the *in vivo* anti-osteoclastogenic and direct anti-tumor effects of IFN-γ in experimental bone metastasis.

We have demonstrated that IFN-γ exerted direct anti-tumor effects on a Tax-expressing tumor cell line, including decreased proliferation, attenuation of ERK phosphorylation, and caspase 3 activation (Fig. 3). *In vivo*, IFN-γ administration to tumor-bearing Tax^{+}IFN-$\gamma^{-/-}$ mice prevented new tumor formation and caused a reduction in tumor cell proliferation as evidenced by decreased BrdUrd incorporation (Fig. 2). Although IFN-γ halted the continued growth of established tumors, no significant reduction in their size was observed. In this study, we also observed decreased growth of a Tax^{+}IFN-$\gamma^{-/-}$ tumor line in mice where the host cells lacked the IFN-γ receptor, providing further evidence to the direct anti-tumor effect of IFN-γ in addition to its indirect anti-angiogenic effects (2). Thus, both direct and indirect actions of IFN-γ on Tax tumor cells contributed to the increased tumor burden in Tax^{+}IFN-$\gamma^{-/-}$ mice.

Although osteoclasts and tumor cells both respond to IFN-γ treatment *in vitro* with decreased cell viability, we cannot make broad conclusions regarding other cells types. The mechanisms accounting for the various cell type-specific responses to IFN-γ are not well understood. For example, cell type-specific expression of downstream target genes may dictate IFN-γ responses. Additionally, mutations in many components of the IFN-γ signaling pathway have been identified in tumor cells, many having consequences on IFN-γ responsiveness (29–31).

Because of the wide range of mutations, single nucleotide polymorphisms, and signaling pathway deregulations observed in tumor cells, tumor cells are not universally sensitive to IFN-γ. However, IFN-γ has also been reported to decrease proliferation of non-Tax-expressing tumors, such as experimental ovarian and neuroendocrine carcinoma cells (4, 24, 25), suggesting that the anti-tumor activity of IFN-γ is not limited to Tax-expressing tumors. Although we

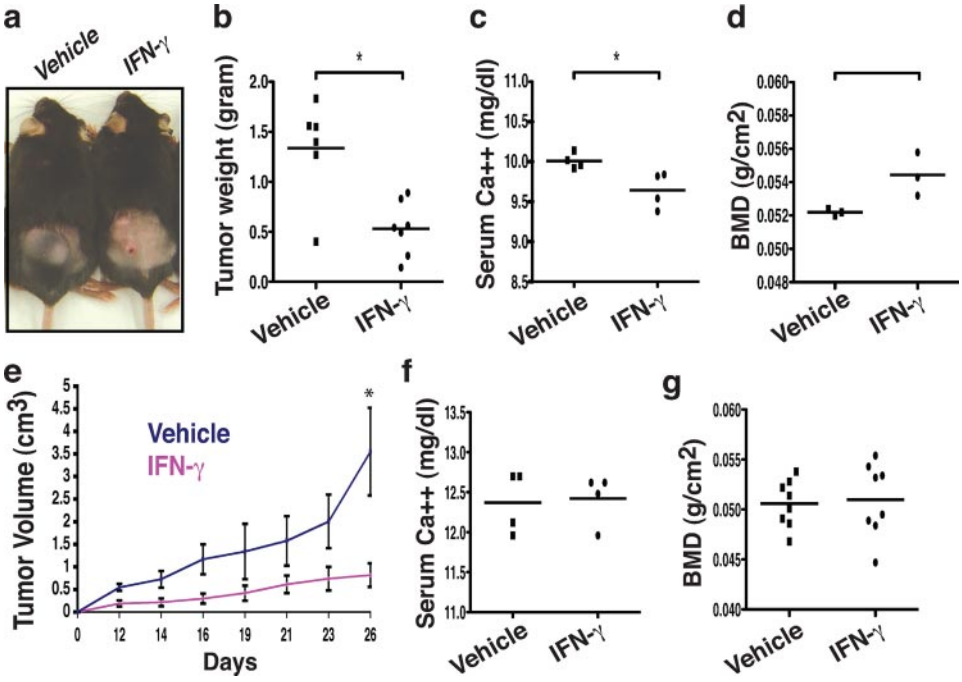

FIGURE 5. **IFN-γ inhibited Tax$^+$ tumor cells *in vivo* and prevented tumor-associated bone loss and hypercalcemia.** *a–d,* immunocompetent C57BL/6 mice were subcutaneously transplanted with TGN tumor cells and treated for 3 weeks with vehicle or recombinant IFN-γ as indicated. *a,* representative picture of subcutaneous TGN tumors at 3 weeks post-transplantation. *b,* IFN-γ treatment decreased the average weight of dissected tumors at 3 weeks (*, $p < 0.01$, ANOVA). $n = 6$ vehicle; $n = 7$ IFN-γ-treated mice. *c,* average serum calcium 3 weeks after TGN subcutaneous implantation and treatment (*, $p < 0.05$, ANOVA). $n = 4$ vehicle; $n = 4$ IFN-γ-treated mice. *d,* BMD as measured by DXA of tibia and femur bones 3 weeks after subcutaneous TGN transplantation and IFN-γ treatment. IFN-γ treatment resulted in decreased loss of BMD (*, $p < 0.05$, ANOVA). $n = 3$ vehicle, $n = 3$ IFN-γ-treated mice. *e–g,* IFN-γR1$^{-/-}$ mice on C57BL/6 background were subcutaneously implanted with TGN cells. All mice were treated with vehicle or recombinant IFN-γ for 3 weeks. *e,* average tumor volume measured using bi-directional caliper measurements ($4/3\pi$·length/2·(width/2)^2). IFN-γ treatment decreased tumor volume by day 26 (*, $p < 0.01$, repeated measures ANOVA). *f,* IFN-γ-R1$^{-/-}$ mice had no significant differences in their serum calcium levels 3 weeks after TGN subcutaneous implantation and treatment with IFN-γ (ANOVA, $n = 4$ vehicle; $n = 4$ IFN-γ treated). *g,* IFN-γ treatment did not significantly alter the BMD of IFN-γ-R1$^{-/-}$ mice as measured by DXA scanning of tibia and femur 3 weeks after TGN cell inoculation.

found that IFN-γ induced STAT1 phosphorylation and inhibited Tax$^+$-expressing tumor cell viability, others have reported that HTLV-1 Tax-expressing T cell leukemias require STAT3, STAT5, and JAK for their proliferation (32). These data highlight the diversity among tumors in JAK/STAT signaling pathways, even those expressing the same oncogene.

Our data support a direct anti-tumor effect of IFN-γ but also identify an additional previously unexplained indirect manner by which host osteoclasts contribute to Tax$^+$ tumor growth. The increased tumor burden observed in Tax$^+$IFN-γ$^{-/-}$ mice and in subcutaneously implanted Tax$^+$ tumor cells was associated with enhanced OC recruitment and activation, increased trabecular bone loss, and elevated serum calcium. We have previously shown that inhibition of OC formation and function decreases osteolytic bone lesions and soft tissue tumors in Tax transgenic mice (17). Likewise, enhancement of OC activity has been shown to enhance tumor burden in bone, partly through OC-mediated release of growth factors stored in the bone matrix during resorption (33, 34). It has also been shown that IFN-γ directly inhibits osteoclastogenesis *in vitro* and that this inhibitory effect is mediated by IFN-γ-induced increased degradation of TRAF-6 protein in RANKL-stimulated bone marrow-derived macrophages (8, 27, 35). *In vivo*, however, the role of IFN-γ in osteoclast biology and pathological bone diseases remains controversial. Mice lacking an intact IFN-γ signaling pathway are more susceptible to collagen-induced arthritis (9–11) and associated bone loss. This could be mediated indirectly through the host immune system rather than by direct targeting of OCs. Recently, Gao *et al.* (12) showed that IFN-γ indirectly stimulates, rather than inhibits, osteoclast formation and bone loss *in vivo* after ovariectomy by stimulating antigen-driven T cell activation. Enhanced osteolytic lesion formation in Tax$^+$IFN-γ$^{-/-}$ mice and the ability of IFN-γ to significantly reduce hypercalcemia and bone loss in tumor-bearing wild type but not IFN-γR1$^{-/-}$ hosts strongly support a direct anti-osteoclastogenic role for IFN-γ in the setting of cancer-induced bone disease.

Unlike patients with autoimmune diseases such as rheumatoid arthritis and T cell-mediated bone loss in postmenopausal osteoporosis (36–38), many cancer patients, particularly those with advanced disease, are in a immunosuppressive state (39–41). Therefore, we hypothesize that the diminished skeletal health and increased tumor-associated bone loss observed in advanced stage cancer patients could be due to a lack of IFN-γ-mediated inhibition of both osteoclasts and tumor cells. Tax$^+$IFN-γ$^{-/-}$ mice reproduce this unique clinical scenario, as *in vivo* IFN-γ deficiency causes enhanced osteolytic lesion formation and increased OC activity when compared with Tax$^+$IFN-γ$^{+/+}$ mice. Further investigations into the role of IFN-γ in bone metastasis and hypercalcemia using other animal models of metastatic diseases such as breast cancer and prostate cancer are warranted.

In this study we also found that IFN-γ negatively regulates M-CSF-mediated proliferation and survival of osteoclast progenitors. This is consistent with previous observations by Xaus *et al.* (42). In addition, Fenton *et al.* (43) showed that primary alveolar macrophages isolated from tuberculosis-infected hosts produce IFN-γ *in vitro*. One possibility is that BMMs isolated from Tax$^+$IFN-γ$^{+/+}$ mice may secrete IFN-γ into the media and subsequently suppress M-CSF-mediated OC survival and proliferation. Conversely, BMM from Tax$^+$IFN-γ$^{-/-}$ are incapable of IFN-γ$^{-/-}$ production, and this may partially account for the differences in the *in vitro* OC formation seen between these two genotypes. Whether

IFN-γ also regulates M-CSF-mediated OC survival and OC differentiation *in vivo* remains to be investigated.

We also observed significant reduction of Tax-expressing tumor cell-induced hypercalcemia and bone loss after IFN-γ treatment. Currently about 10–30% of cancer patients develop humeral hypercalcemia of malignancy (HHM), and there are few effective treatments to prevent this serious complication. Furthermore, some cancer patients with HHM are refractory to bisphosphonate treatment because of parathyroid hormone-related protein (PTHrP)-stimulated calcium reabsorption in renal tubules (44). Because PTHrP-producing tumor cells are major culprits of HHM, direct targeting of tumor cells decreases their PTHrP secretion. In addition to direct inhibitory effects on osteoclasts, IFN-γ may play a unique role both for the prevention and treatment for patients with HHM. We are currently investigating the hypercalcemia-associated humoral factors secreted by Tax-expressing tumor cells and the specific effects of IFN-γ treatment on these factors.

In conclusion, we have shown that, in addition to its direct anti-tumor effects, IFN-γ also suppresses tumor-induced bone loss and hypercalcemia in Tax^+ mice. IFN-γ mediates these effects by directly targeting host OCs to inhibit osteolysis. These data suggest a protective role for IFN-γ that warrants additional research into novel therapeutic treatments for patients with bone metastases and hypercalcemia of malignancy.

Acknowledgments—We thank members of the Weilbaecher lab and Drs. Steven Teitelbaum, Paddy Ross, Robert Schreiber, Lee Ratner, Michael Tomasson, and Valerie Salazar for helpful discussions. We thank Dr. Deb Novak for help with quantification of in vivo BrdUrd labeling. We thank Drs. Nadella, Wellman, Weisbrode, and Stromberg from Ohio State University for reviewing pathology slides of tumor transplantation studies. We thank Crystal Idleburg, Devra Blanden, Stefan Niewiesk, Stephanie Baker, Elyse Cohen, and Angie Hirbe for technical assistance. We thank Trey Coleman and the Center for Nutrition Research Unit for assistance with DXA scanning supported by National Institutes of Health Grant DK56341. Finally we thank Julie Prior and David Piwnica-Worms of the Molecular Imaging Center (supported by National Institutes of Health Grant P50 CA 94056).

REFERENCES

1. Dunn, G. P., Koebel, C. M., and Schreiber, R. D. (2006) *Nat. Rev. Immunol.* **6,** 836–848
2. Mitra-Kaushik, S., Harding, J., Hess, J., Schreiber, R., and Ratner, L. (2004) *Blood* **104,** 3305–3311
3. Ikeda, H., Old, L. J., and Schreiber, R. D. (2002) *Cytokine Growth Factor Rev.* **13,** 95–109
4. Detjen, K. M., Farwig, K., Welzel, M., Wiedenmann, B., and Rosewicz, S. (2001) *Gut* **49,** 251–262
5. Kakuta, S., Tagawa, Y., Shibata, S., Nanno, M., and Iwakura, Y. (2002) *Immunology* **105,** 92–100
6. Tannir, N., Jonasch, E., Pagliaro, L. C., Mathew, P., Siefker-Radtke, A., Rhines, L., Lin, P., Tibbs, R., Do, K. A., Lin, S. H., and Tu, S. M. (2006) *Cancer* **107,** 497–505
7. Teitelbaum, S. L. (2007) *Am. J. Pathol.* **170,** 427–435
8. Takayanagi, H., Ogasawara, K., Hida, S., Chiba, T., Murata, S., Sato, K., Takaoka, A., Yokochi, T., Oda, H., Tanaka, K., Nakamura, K., and Taniguchi, T. (2000) *Nature* **408,** 600–605
9. De Klerck, B., Carpentier, I., Lories, R. J., Habraken, Y., Piette, J., Carmeliet, G., Beyaert, R., Billiau, A., and Matthys, P. (2004) *Arthritis Res. Ther.* **6,** R220–R231
10. Chu, C. Q., Song, Z., Mayton, L., Wu, B., and Wooley, P. H. (2003) *Ann. Rheum. Dis.* **62,** 983–990
11. Vermeire, K., Heremans, H., Vandeputte, M., Huang, S., Billiau, A., and Matthys, P. (1997) *J. Immunol.* **158,** 5507–5513
12. Gao, Y., Grassi, F., Ryan, M. R., Terauchi, M., Page, K., Yang, X., Weitzmann, M. N., and Pacifici, R. (2007) *J. Clin. Investig.* **117,** 122–132
13. Key, L. L., Jr., Rodriguiz, R. M., Willi, S. M., Wright, N. M., Hatcher, H. C., Eyre, D. R., Cure, J. K., Griffin, P. P., and Ries, W. L. (1995) *N. Engl. J. Med.* **332,** 1594–1599
14. Hochman, N., Hojo, H., Hojo, S., Corcoran, M. L., Allen, J. B., Hansen, C. T., Wahl, S. M., and Wahl, L. M. (1991) *Cell. Immunol.* **137,** 14–23
15. Madyastha, P. R., Yang, S., Ries, W. L., and Key, L. L., Jr. (2000) *J. Interferon Cytokine Res.* **20,** 645–652
16. Grossman, W. J., Kimata, J. T., Wong, F. H., Zutter, M., Ley, T. J., and Ratner, L. (1995) *Proc. Natl. Acad. Sci. U. S. A.* **92,** 1057–1061
17. Gao, L., Deng, H., Zhao, H., Hirbe, A., Harding, J., Ratner, L., and Weilbaecher, K. (2005) *Blood* **106,** 4294–4302
18. Tintut, Y., Parhami, F., Tsingotjidou, A., Tetradis, S., Territo, M., and Demer, L. L. (2002) *J. Biol. Chem.* **277,** 14221–14226
19. Hirbe, A. C., Uluçkan, O., Morgan, E. A., Eagleton, M. C., Prior, J. L., Piwnica-Worms, D., Trinkaus, K., Apicelli, A., and Weilbaecher, K. (2007) *Blood* **109,** 3424–3431
20. Bakewell, S. J., Nestor, P., Prasad, S., Tomasson, M. H., Dowland, N., Mehrotra, M., Scarborough, R., Kanter, J., Abe, K., Phillips, D., and Weilbaecher, K. N. (2003) *Proc. Natl. Acad. Sci. U. S. A.* **100,** 14205–14210
21. Tanaka, Y., Yoshida, A., Takayama, Y., Tsujimoto, H., Tsujimoto, A., Hayami, M., and Tozawa, H. (1990) *Jpn. J. Cancer Res.* **81,** 225–231
22. Natasha, T., Kuhn, M., Kelly, O., and Rittling, S. R. (2006) *Am J. Pathol.* **168,** 551–561
23. Zhao, H., Kitaura, H., Sands, M. S., Ross, F. P., Teitelbaum, S. L., and Novack, D. V. (2005) *J. Bone Miner. Res.* **20,** 2116–2123
24. Kim, E. J., Lee, J. M., Namkoong, S. E., Um, S. J., and Park, J. S. (2002) *J. Cell. Biochem.* **85,** 369–380
25. Detjen, K. M., Kehrberger, J. P., Drost, A., Rabien, A., Welzel, M., Wiedenmann, B., and Rosewicz, S. (2002) *Int. J. Oncol.* **21,** 1133–1140
26. Favata, M. F., Horiuchi, K. Y., Manos, E. J., Daulerio, A. J., Stradley, D. A., Feeser, W. S., Van Dyk, D. E., Pitts, W. J., Earl, R. A., Hobbs, F., Copeland, R. A., Magolda, R. L., Scherle, P. A., and Trzaskos, J. M. (1998) *J. Biol. Chem.* **273,** 18623–18632
27. Fox, S. W., and Chambers, T. J. (2000) *Biochem. Biophys. Res. Commun.* **276,** 868–872
28. Huang, W., O'Keefe, R. J., and Schwarz, E. M. (2003) *Arthritis Res. Ther.* **5,** R49–R59
29. Dunn, G. P., Sheehan, K. C., Old, L. J., and Schreiber, R. D. (2005) *Cancer Res.* **65,** 3447–3453
30. Lee, K. Y., Geng, H., Ng, K. M., Yu, J., van Hasselt, A., Cao, Y., Zeng, Y. X., Wong, A. H., Wang, X., Ying, J., Srivastava, G., Lung, M. L., Wang, L. D., Kwok, T. T., Levi, B. Z., Chan, A. T., Sung, J. J., and Tao, Q. (2008) *Oncogene* **27,** 5267–5276
31. Kaplan, D. H., Shankaran, V., Dighe, A. S., Stockert, E., Aguet, M., Old, L. J., and Schreiber, R. D. (1998) *Proc. Natl. Acad. Sci. U. S. A.* **95,** 7556–7561
32. Tomita, M., Kawakami, H., Uchihara, J. N., Okudaira, T., Masuda, M., Matsuda, T., Tanaka, Y., Ohshiro, K., and Mori, N. (2006) *Retrovirology* **3,** 22
33. Hirbe, A. C., Rubin, J., Uluckan, O., Morgan, E. A., Eagleton, M. C., Prior, J. L., Piwnica-Worms, D., and Weilbaecher, K. N. (2007) *Proc. Natl. Acad. Sci. U. S. A.* **104,** 14062–14067
34. Mundy, G. R. (2002) *Nat. Rev. Cancer* **2,** 584–593
35. Takahashi, N., MacDonald, B. R., Hon, J., Winkler, M. E., Derynck, R., Mundy, G. R., and Roodman, G. D. (1986) *J. Clin. Investig.* **78,** 894–898
36. Toh, M. L., and Miossec, P. (2007) *Curr. Opin. Rheumatol.* **19,** 284–288
37. Zhu, L., Ji, F., Wang, Y., Zhang, Y., Liu, Q., Zhang, J. Z., Matsushima, K., Cao, Q., and Zhang, Y. (2006) *J. Immunol.* **177,** 8226–8233

38. Wan, B., Nie, H., Liu, A., Feng, G., He, D., Xu, R., Zhang, Q., Dong, C., and Zhang, J. Z. (2006) *J. Immunol.* **177,** 8844–8850
39. Cochran, A. J., Wen, D. R., Farzad, Z., Stene, M. A., McBride, W., Lana, A. M., Hoon, D. S., and Morton, D. L. (1989) *Anticancer Res.* **9,** 859–864
40. Kim, R., Emi, M., and Tanabe, K. (2007) *Immunology* **121,** 1–14
41. Merchant, M. S., Melchionda, F., Sinha, M., Khanna, C., Helman, L., and Mackall, C. L. (2007) *Cancer Immunol. Immunother.* **56,** 1037–1046
42. Xaus, J., Cardo, M., Valledor, A. F., Soler, C., Lloberas, J., and Celada, A. (1999) *Immunity* **11,** 103–113
43. Fenton, M. J., Vermeulen, M. W., Kim, S., Burdick, M., Strieter, R. M., and Kornfeld, H. (1997) *Infect. Immun.* **65,** 5149–5156
44. Weissglas, M., Lowik, C., Schamhart, D., Theuns, H., Kurth, K. H., and Papapoulos, S. (2007) *BJU Int.* **99,** 1530–1533

Interferon-γ Targets Cancer Cells and Osteoclasts to Prevent Tumor-associated Bone Loss and Bone Metastases

Zhiqiang Xu, Michelle A. Hurchla, Hongju Deng, Özge Uluçkan, Fang Bu, Andrew Berdy, Mark C. Eagleton, Emanuela A. Heller, Desiree H. Floyd, Wessel P. Dirksen, Sherry Shu, Yuetsu Tanaka, Soledad A. Fernandez, Thomas J. Rosol and Katherine N. Weilbaecher

J. Biol. Chem. 2009, 284:4658-4666.
doi: 10.1074/jbc.M804812200 originally published online December 5, 2008
